chemosensors

MDPI

Article

Fluorescent "OFF–ON" Sensors for the Detection of Sn^{2+} Ions Based on Amine-Functionalized Rhodamine 6G

Balamurugan Rathinam [1], Vajjiravel Murugesan [2] and Bo-Tau Liu [1,*]

[1] Department of Chemical and Materials Engineering, National Yunlin University of Science and Technology, Yunlin 64002, Taiwan; balar@yuntech.edu.tw
[2] Department of Chemistry, B.S. Abdur Rahman Crescent Institute of Science and Technology, Chennai 600 048, India; vajjiravel_m@crescent.education
* Correspondence: liubo@yuntech.edu.tw; Tel.: +886-5-534-2601; Fax: +886-5-531-2071

Abstract: These structurally isomeric rhodamine 6G-based amino derivatives are designed to detect Sn^{2+} ions. The receptors exhibit rapid fluorescent "turn-on" responses towards Sn^{2+}. The absorption (530 nm) and fluorescent intensity (551 nm) of the receptors increase when increasing the concentration of Sn^{2+}. The hydrazine derivative exhibits more rapid sensitivity towards Sn^{2+} than the ethylene diamine derivative, indicating that the presence of an alkyl chain in the diamine decreases the sensitivity of the receptors towards Sn^{2+}. The presence of carbonyl groups and terminal amino groups strongly influences the sensitivity of the chemosensors toward Sn^{2+} by a spirolactam ring-opening mechanism. The receptors exhibit 1:1 complexation with Sn^{2+} as evidenced by Job plot, and the corresponding limit of detection was found to be 1.62×10^{-7} M. The fluorescence images of the receptors and their complexes reveal their potential applications for imaging of Sn^{2+} in real/online samples.

Keywords: fluorescent sensor; stannous ion; rhodamine 6G; OFF–ON fluorescent receptor; metal coordination

Citation: Rathinam, B.; Murugesan, V.; Liu, B.-T. Fluorescent "OFF–ON" Sensors for the Detection of Sn^{2+} Ions Based on Amine-Functionalized Rhodamine 6G. *Chemosensors* **2022**, *10*, 69. https://doi.org/10.3390/chemosensors10020069

Academic Editors: Jeroen Missinne, Geert Van Steenberge and Thomas Geernaert

Received: 24 January 2022
Accepted: 6 February 2022
Published: 9 February 2022

1. Introduction

Tin is a grey-white metal and exists in Sn^{2+} and Sn^{4+} oxidation states. The concentration of tin in soil and Earth's crust is approximately <1 to 220 mg/kg and 2–3 mg/kg, respectively. Tin can be used in electrical/electronic and industrial applications such as reducing agents, protective coating for food containers, manufacturing of metallized glazing, and preventive dentistry (tin(II) fluoride). Tin deficiency increases the risk of poor growth, cancer prevention, and hearing loss [1,2]. Exposure to different tin forms causes gastrointestinal symptoms such as abdominal cramps, vomiting, diarrhea, skin and nasal irritation. Certain studies on laboratory animals involving oral administration have revealed that tin(II) chloride has significant tissue effects on the kidney, liver, pancreas, testis, and brain [3–5]. Accordingly, exploring a facile, sensitive, and highly selective Sn^{2+} detection method is necessary.

Fluorescence "OFF–ON" and "ON–OFF" sensing techniques are more cost-efficient than traditional analyses, such as inductively coupled plasma-mass spectrometry, atomic absorption spectroscopy, and inductively coupled plasma-atomic emission spectrometry, due to their rapid performance, non-destructive method, and high sensitivity [6–11]. Recently, many efforts have been devoted to developing fluorescent sensors for Sn^{2+}/Sn^{4+}, which are based on naphthalimide–rhodamine B [2], coumarin derivative [12], oxo chromene-functionalized rhodamine B [13], alkene-functionalized rhodamine B [14], diarylethene-carbazole derivative [15], 4-(naphthalen-1-ylethynyl) aniline appended rhodamine B [16], benzyl 3-aminopropanoate–rhodamine B conjugate [17], rhodamine B and N,N-bis-(2-hydroxyethyl)ethylenediamine or tert-butyl carbazate derivatives [18], naphthoquinone-dopamine [19], benzophenone derivative [20], 4-((3-chloro-1,4-dioxo-1,4-dihydronaphthalen-

2-yl)amino)benzenesulfonamide [21], 5-(4-(diphenylamino)phenyl)picolinaldehyde derivative [22], rhodamine-thio derivative [23], europium complexes based on 2-(3,5-dimethoxyphenyl)-1H-imidazo[4,5-f][1,10]phenanthroline [24], and citrate stabilized silver nanoparticles [25]. Among them, most sensors have complex structures and need multi-step synthesis. An easy-to-fabricate and efficient Sn^{2+} fluorescent receptor is highly desired to explore in this context.

Rhodamine derivatives are extensively used as fluorescent sensors for the selective detection of metal ions such as Cu^{2+} [26–28], Fe^{3+} [27,29,30], Pd^{2+} [10,11,27], Zn^{2+} [7,31], Al^{3+} [32], Hg^{2+} [33], and Cr^{3+} [34] due to their great photo-physical properties, including photostability and excellent quantum yields. In this work, we are the first to present rhodamine 6G-based amino derivatives that exhibit higher sensitivity towards Sn^{2+} at pH 6.8 over the other metals studied. The amine-functionalized rhodamine probes were prepared by a facile, easy-to-synthesize, and cost-effective method. The binding mechanism, limit of detection (LOD), and fluorescence imaging studies are discussed in detail. In addition, the potential of the probe was demonstrated by determining the amount of tin present in the $SnCl_2$ catalyzed reduction product as an impurity.

2. Experimental Section

2.1. Materials and Methods

Rhodamine 6G and metal ions were purchased from Sigma-Aldrich and used as received. Hydrazine hydrate and ethylene diamine were purchased from Merck and used without further purification. Dichloromethane and THF were purified before use. All the solvents used for the syntheses were spectrophotometric grade. Nuclear magnetic resonance (NMR) spectra were obtained from a Bruker AMX-500 high-resolution NMR spectrometer in deuterated solvents. UV/Vis absorption spectra were measured by a Jasco V-770 spectrophotometer. Fourier transform infrared (FTIR) spectra were measured by a PerkinElmer Spectrum One FTIR spectrophotometer. The fluorescence spectra were measured with a Horiba Fluoromax-4 fluorescence spectrophotometer at excitation wavelength = 510 nm. The receptors were mixed with metal ion solutions for 15 min to measure the optical responses. Fluorescent imaging of receptors and their complexes with Sn^{2+} coated in glass plates was recorded by a Nikon Cl confocal unit equipped with argon 488 and He-Ne 543 lasers and an EZ-C1 digital camera.

2.2. Synthesis and Characterization of Receptors

Rhodamine 6G-diamine derivative was synthesized as reported elsewhere [35]. Briefly, 4.8 g of rhodamine 6G and 100 mL of ethanol were mixed in a 250 mL flask. Fifteen milliliters of hydrazine hydrate was added into the solution drop-wise. After that, the mixture was refluxed overnight. The resulting solution was cooled to room temperature, and then its solvent was removed by a rotary evaporator. The crude solid was extracted by dichloromethane, then washed with water and HCl to remove residual hydrazine. Finally, the solution was adjusted to neutral by 1 M NaOH. In this way, the excess amines were eliminated from the product. The crude was dried with anhydrous magnesium sulfate to obtain a half-white solid (Rh-Hyd). From the TLC, a single spot was observed through the mobile phase of ethyl acetate:hexane = 3:1, indicating the purity of the samples. Because rhodamine is a colored compound and the resulting derivatives are white to half-white solids, there may be no starting compound in the product. The purity was also evaluated by mass spectrum analysis. For comparison, diamines with different alkyl chains were also synthesized. The rhodamine 6G–ethylene diamine derivative (Rh-ED) was synthesized according to the same procedure, except that ethylene diamine was used in place of hydrazine hydrate. All the results of ^{1}H-NMR and ^{13}C-NMR are in accordance with the structure of the compound. Both receptors were found to be soluble in ethanol, acetonitrile, chlorinated solvents, and high polar solvents such as DMF and DMSO. Moreover, they can also be dissolved in a mixture of ethanol:water (8:2, v/v). All UV-Vis and fluorescent

spectra were measured in a mixture of C_2H_5OH:H_2O (8:2, *v*/*v*) at 25 °C at pH 6.8, unless otherwise mentioned.

Rh-Hyd: Yield = 76%. ^{1}H-NMR ($CDCl_3$, δ in ppm): 1.18–1.28 (t, 6H, NCH_2CH_3), 1.92 (s, 6H, Ar-CH_3), 3.27–3.45 (s, 4H, NCH_2CH_3), 3.69–3.73 (b, 2H, $ArNHCH_2$), 6.26 (s, 2H, ArH), 6.55 (s, 2H, ArH), 7.05 (d, 2H, ArH), 7.42–7.51 (m, 2H, ArH), 7.97 (d, 1H, ArH). ^{13}C-NMR (CDCl3, δ in ppm): 14.58 (NCH_2CH_3), 16.70 (Ar-CH_3), 38.61(NCH_2CH_3), 65.96 (spiro C), 118.27 (ArC-C-spiro), 123.02 (ArC-CH_3), 123.77 (ArC-C=O), 127.75 (ArC-C-C=O), 128.14 (ArC), 129.76 (ArC), 132.59 (ArC), 147.07 (ArC-spiro C), 151.64 (ArC-NH), 152.11 (ArC-O), 166.20 (C=O).

Rh-ED: Yield = 87%. ^{1}H-NMR ($CDCl_3$, δ in ppm): 1.16–1.29 (t, 6H, NCH_2CH_3), 1.92 (s, 6H, Ar-CH_3), 2.31 (s, 6H, -CH_2-NH_2), 3.09–3.12 (N-CH_2), 3.19 (s, 4H, NCH_2CH_3), 3.57–3.62 (b, 2H, $ArNHCH_2$), 6.24 (s, 2H, ArH), 6.33 (s, 2H, ArH), 7.0 (d, 2H, ArH), 7.43–7.47 (m, 2H, ArH), 7.84 (d, 1H, ArH). ^{13}C-NMR ($CDCl_3$, δ in ppm): 15.09 (NCH_2CH_3), 17.10 (Ar-CH_3), 39.06 (NCH_2CH_3), 41.09 (CH_2-NH_2), 42.63 (CH_2-CH_2-NH_2), 66.00 (spiro C), 118.96 (ArC-C-spiro), 123.39 (ArC-CH_3), 124.26 (ArC-C=O), 128.75 (ArC-C-C=O), 131.46 (ArC), 133.19 (ArC), 148.40 (ArC-spiro C), 152.35 (ArC-NH), 154.59 (ArC-O), 169.54 (C=O).

3. Results and Discussion

The structures of the synthesized receptors are shown in Scheme 1. The receptors were prepared from the amination of rhodamine 6G with hydrazine hydrate or ethylene diamine in ethanol solution. The receptors were characterized by ^{1}H-NMR and ^{13}C-NMR analyses. All the spectra are shown in Figures S1–S4. The ^{1}H-NMR spectrum of Rh-Hyd in $CDCl_3$ is shown in Figure S1. The aromatic protons of the Rh-Hyd present between 6.57 to 7.97 ppm. The methyl protons linked to the benzene ring of the rhodamine unit are at 1.92 ppm. The presence of a peak at 3.69 ppm corresponds to –NH protons directly attached to the benzene ring. Peaks at 3.27 and 1.18 ppm correspond to the protons of CH_2 and CH_3 protons associated with the Ar-NH- group, respectively. Figure S2 shows that all of the aromatic carbons of Rh-Hyd appear around 118–132 ppm in the ^{13}C-NMR spectrum. The aromatic carbons linked to –NH and -O present at 151 and 152 ppm, respectively. The carbon bridging two heterocyclic rings appears at 65.9 ppm. All of the aliphatic carbons present near 14.5–16.7 ppm. The carbon for the C=O- group of the rhodamine unit is at 166 ppm. The Rh-Hyd mass spectrum was recorded in Figure S5. We observed the same molecular weight of the compound ($C_{26}H_{28}N_4O_2$) as expected (428.2), indicating the high purity of the compound. Figures S3 and S4 show the ^{1}H-NMR spectrum and ^{13}C-NMR spectrum of Rh-ED, respectively. All of the values in the spectra correspond well to the receptor's structure.

3.1. Binding Properties of the Synthesized Receptors

The solution of all the receptors in the mixture of C_2H_5OH:H_2O = 8:2 (*v*/*v*) displayed no color and no fluorescence, implying that receptors exist in the closed-ring form of spirolactam [36]. The chelation of the two receptors to Sn^{2+} was evaluated by the fluorescent titrations. The titration experiments showed that the emission intensity increased gradually with the addition of Sn^{2+} up to 50 equivalents (Figure 1). The color of both solutions resulted in a brilliant pinkish-orange, which was accompanied by a spirolactam-ring opening of the rhodamine unit. Sn^{2+} addition led to an emission peak at 551 nm in the fluorescent spectra. Under the addition of 2-equivalent Sn^{2+}, the fluorescent intensity of the Rh-Hyd and Rh-ED solution was enhanced by ca.14 and 11 folds respectively when compared with their blanks. The LOD of the receptors can be calculated from the equation LOD = K × Sb1/S, where K = 3.3, S is the slope of the calibration curve, and Sb1 is the standard deviation of the blank solution. The LOD for Rh-Hyd and Rh-ED can be calculated as 1.62×10^{-7} and 3.24×10^{-7} M, respectively. The time-dependent fluorescent study revealed that the fluorescence maximum was obtained after nearly 15 min of Sn^{2+} addition for the Rh-Hyd, whereas the Rh-ED took more than 40 min to reach stability (Figure 2). According to the

above analyses, Rh-Hyd exhibits more rapid response and higher sensitivity toward Sn^{2+} than Rh-ED. Thus, Rh-Hyd is a better probe for the detection of Sn^{2+}.

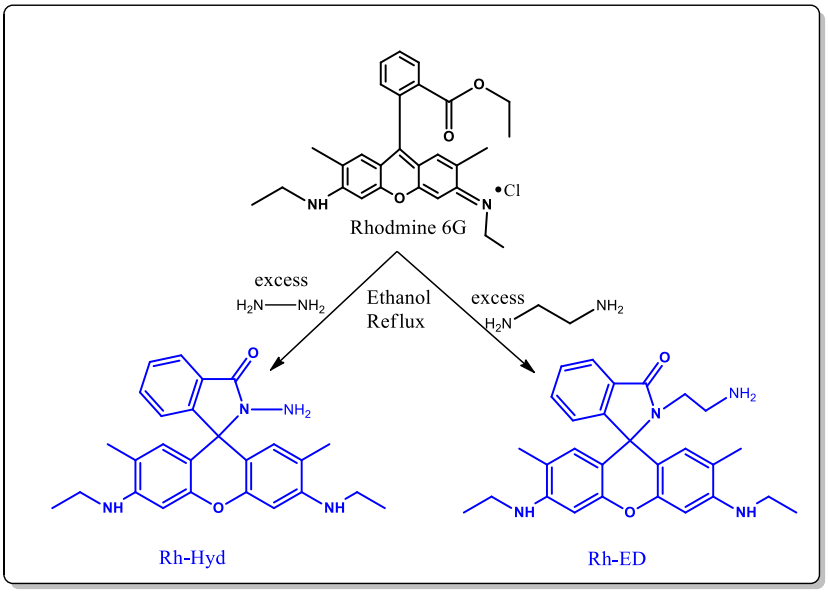

Scheme 1. Synthesis of receptors.

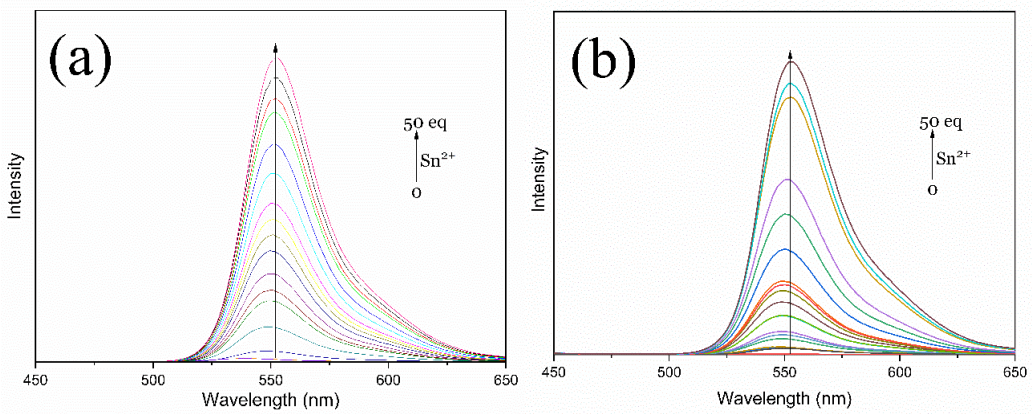

Figure 1. Changes in the emission spectra of (**a**) Rh-Hyd and (**b**) Rh-ED (10^{-6} M) at pH = 6.9 upon titration with various Sn^{2+} equivalents (0, 1, 2, 3, 4, 5, 6, 7, 8, 9, 10, 15, 20, 25, 30, 40, 50).

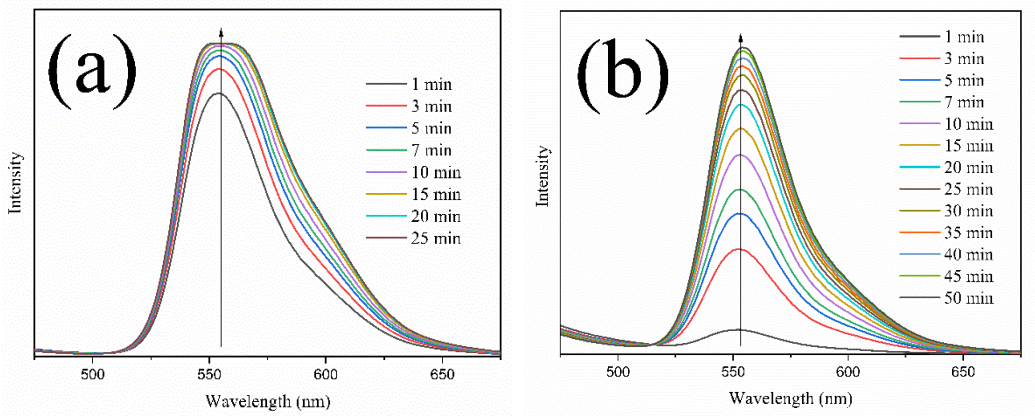

Figure 2. Time-dependent PL spectra of Rh-Hyd (**a**) and Rh-ED (**b**) with 10 equivalents of Sn^{2+} in C_2H_5OH:H_2O (8:2, *v*/*v*).

In order to verify the selectivity of the receptor, the perchlorate, nitrate, acetate or chlorate salts of different metal ions such as Ag^+, Cu^{2+}, Fe^{2+}, K^+, Li^+, Na^+, Ni^{2+}, Pb^{2+}, and Zn^{2+} in a mixture of C_2H_5OH:H_2O (8:2, *v*/*v*) at room temperature at pH 6.8 were employed in the fluorescent experiments. Each metal solution was mixed with the receptor for 15 min and then recorded for the spectra of its complexes. After treating with 10 equivalents of metal ions, the receptor (10^{-7} M) exhibited strong fluorescence at 551 nm (Figure 3a), and strong absorption at 530 nm (Figure 3b) accompanied with a color change from colorless to bright pinkish orange only for Sn^{2+}. No significant absorption or emission enhancement was promoted by the other metal ions. Observing the real images of the receptor with different metal ions under UV light (Figure 3c), it can be seen that the solutions did not fluoresce except for Sn^{2+}, which is consistent with the photoluminescence analysis. This result indicates that the receptor has high selectivity towards Sn^{2+}. Different sources of metal ions were also tested. For example, we used copper chloride, copper nitrate, and copper sulfate for Cu^{2+}, and iron chloride and iron nitride for Fe^{3+}. These changes in metal ion sources only showed variations in color. There were no apparent changes observed in the fluorescence spectra, indicating that counter-ions have insignificant effects on this receptor. However, other metal ions (co-ions) should still be taken into account in physiological applications. The presence of other competitive metal ions such as Ag^+, Cu^{2+}, Fe^{3+}, Na^+, Li^+, Pb^{2+}, Pd^{2+}, Ni^{2+}, and Zn^{2+} were investigated in the optical changes of the receptor. We executed the titrations in a dual metal system to examine the interference of co-cations. The variations in the fluorescent intensity were recorded when other metal ions were added into the receptor-Sn^{2+} solution, as shown in Figure 4. The interferent ion tests revealed that the fluorescent intensity of Rh-Hyd-Sn^{2+} was not influenced significantly by other metal ions. Moreover, amine-functionalized rhodamine 6G derivatives have been reported as a fluorescent sensor for Hg^{2+} [37]. Rh-Hyd exhibited pinkish-orange coloration immediately upon Sn^{2+} addition, whereas the receptor initially showed yellow color and then slowly changed to pinkish-orange color for Hg^{2+} addition. Thus, Sn^{2+} and Hg^{2+} can be distinguished by Rh-Hyd based on naked eye detection.

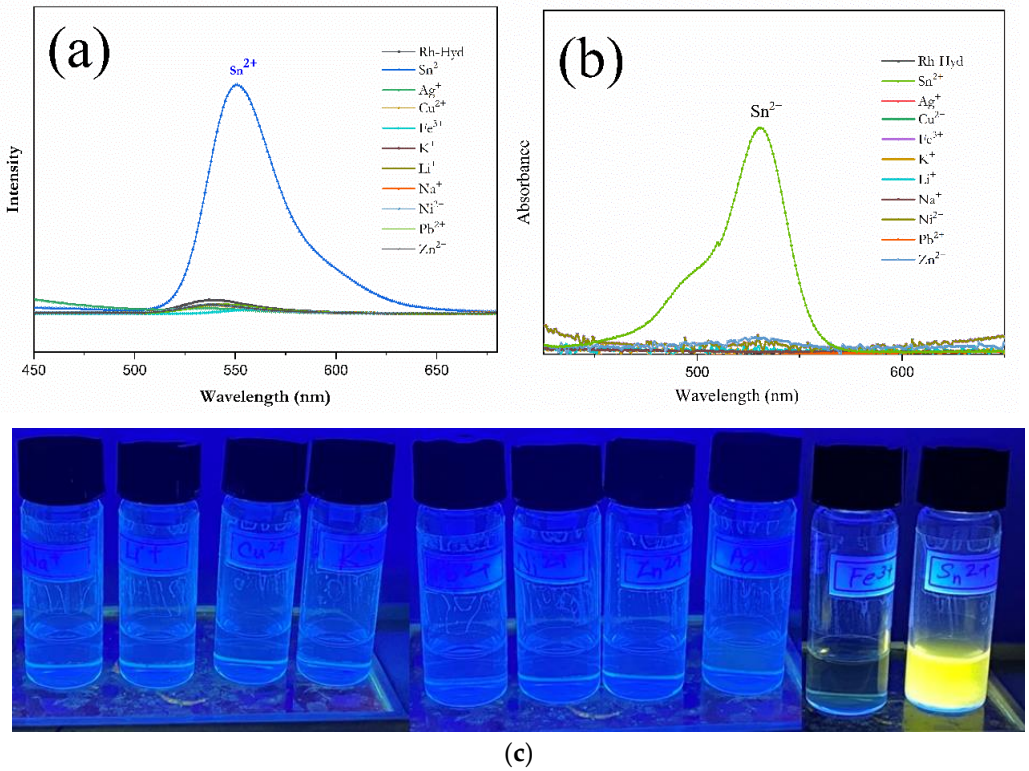

Figure 3. Fluorescent emissions (**a**), UV-Vis absorbances (**b**), and UV-irradiated images (**c**) of Rh-Hyd (10^{-7} M) upon addition of various metal ions.

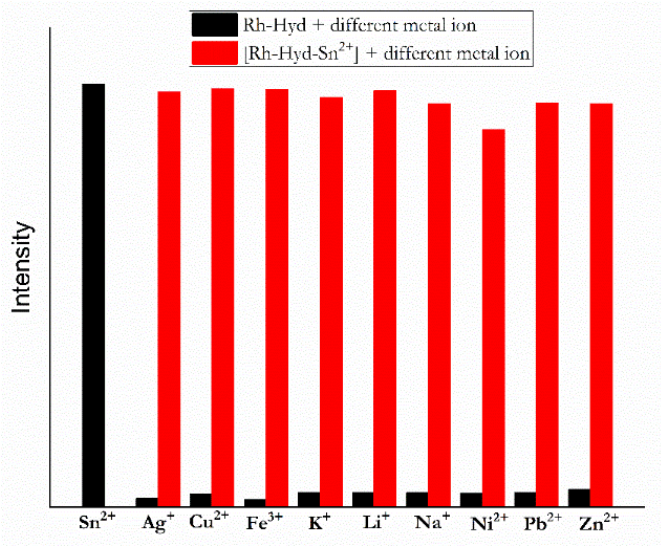

Figure 4. Fluorescent intensity of Rh-Hyd at 551 nm in single metal ion solutions (black bar) and mixtures of Sn^{2+} and other metal ions (red bar).

3.2. Binding Mechanism of the Receptors towards Sn^{2+}

Figure 5 displays the Job plot for the UV-Vis absorption with respect to the ratio of Sn^{2+} to Rh-Hyd. The most preferred coordination structure appears at Sn^{2+}/Rh-Hyd-Sn^{2+} ~0.5. It was demonstrated that the receptor coordinates with Sn^{2+} in a 1:1 stoichiometry. The acid-base titration experiments revealed that the receptor displayed high absorbance at low pH value but no absorbance at pH > 6 (Figure 6). The results imply that the receptor exists in the closed spirolactam form in a neutral/basic medium, whereas the spirolactam ring of the rhodamine unit opens in a strongly acidic solution. The actual pH of the receptor solution is 6.8, and the receptor solution is colorless and non-fluorescent, implying that the receptor remains in the closed spirolactam form initially. The Sn^{2+} addition makes the receptor solution colored and fluorescent, but does not change its pH value. The results reveal that the Sn^{2+} may open the spirolactam ring of the receptor. To further realize the coordination mechanism of the receptors with Sn^{2+}, the receptors and their corresponding complexes (1:1 ratio of receptor to metal ion) were analyzed by FTIR, ^{1}H-NMR, and ^{13}C-NMR spectra. The FTIR spectra of Rh-Hyd and Rh-Ed and their Sn^{2+} complexes are shown in Figure 7 and Figures S6–S9. Rh-Hyd and Rh-ED exhibit the "C=O" group of amide stretching vibration at ~1692 and ~1689 cm^{-1}, respectively, whereas they are significantly shifted to ~1648 cm^{-1} for Sn^{2+} complexation. Similarly, the NH stretching at ~3429 and ~3484 cm^{-1} for Rh-Hyd and Rh-ED were significantly shifted to ~3357 and ~3340 cm^{-1}, respectively, after Sn^{2+} addition. Moreover, significant shifting of the C-N stretching and out-of-plane wagging around ~1198 and ~744 cm^{-1} for Rh-Hyd and ~1201 and ~686 cm^{-1} for Rh-Ed, respectively, indicated that the carbonyl and amino groups are involved in the complexation with Sn^{2+}. Regarding ^{1}H-NMR spectra, the peak at 2.34 ppm corresponding to CH_2 protons attached with amine (-CH_2-NH_2) in Rh-ED (Figure S3) was shifted to 2.76 ppm (Figure S8) after Sn^{2+} complexation. There were no other remarkable changes observed in either the ^{1}H-NMR or ^{13}C-NMR spectra of the receptors for the Sn^{2+} addition. This reveals that the addition of Sn^{2+} did not contribute to any structural changes in the receptors. This evidence suggests that the -C=O and -NH_2 of the receptors lead to a highly coordinated structure with Sn^{2+} and form 1:1 complexes (Figure 8), which exhibit high fluorescence. The fact that Rh-Hyd features a more rapid response and higher sensitivity than Rh-ED may be due to the steric hindrance of the alkyl chain to Sn^{2+} coordination and the higher nucleophilicity of hydrazine than ethylene diamine.

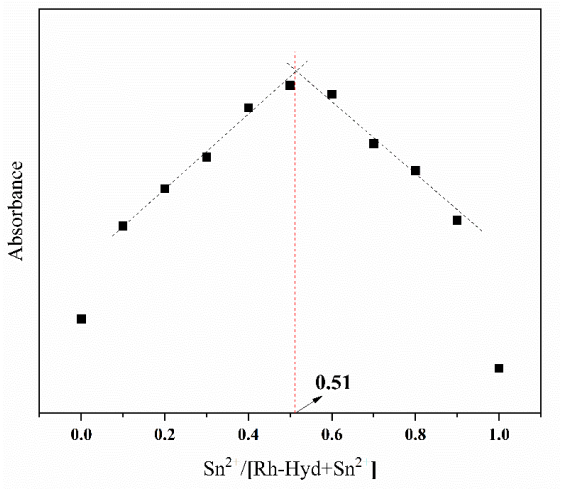

Figure 5. Job plot for Rh-Hyd-Sn^{2+} complexes.

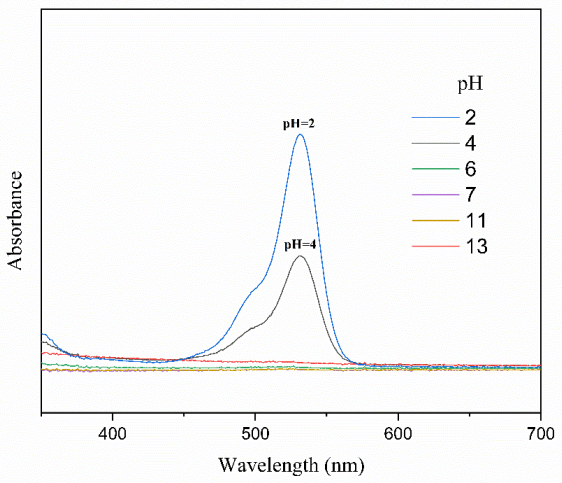

Figure 6. UV-Vis absorption spectra of Rh-Hyd in different pH values.

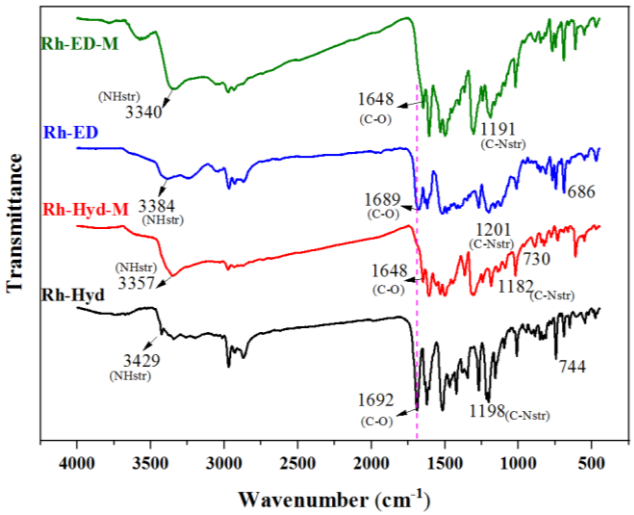

Figure 7. FTIR spectra of the Rh-Hyd, Rh-ED, and their corresponding complexes with metal (M = Sn^{2+} complexes).

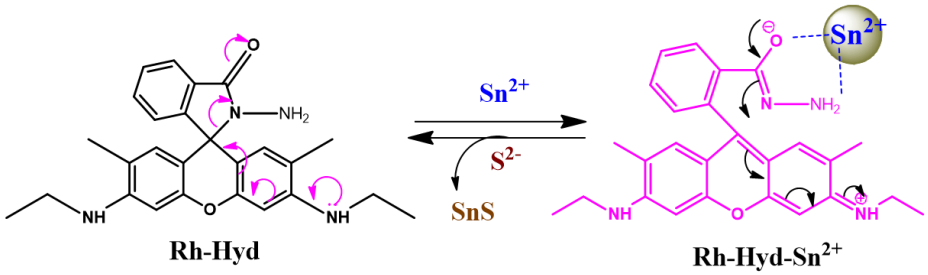

Figure 8. Schematic representation of the possible mechanism for the fluorescent changes of Rh-Hyd with Sn^{2+} addition and reversible binding in the presence of S^{2-}.

3.3. Reversibility of the Receptors

The reversibility of fluorescent sensors to regenerate the free ones from the complex is a significant factor in practical applications. To examine the reversibility of receptors, sodium sulfide (S^{2-}) (1 mM) was considered as a suitable counter ligand to the complex [38]. The absorption and emission spectra of Rh-Hyd-Sn^{2+} solution before and after the addition of S^{2-} were examined. The addition of S^{2-} turned the solution colorless and switched "OFF" the fluorescence. The addition of S^{2-} returned the fluorescent emission to a blank (Figure 9), indicating that the cyclic lactam form of Rh-Hyd was regenerated. This implies that the complexation of sulfide with Sn^{2+} is much stronger than with Rh-Hyd, which leads to the removal of Sn^{2+} from Rh-Hyd through the formation of SnS_2 as grey-colored precipitate, suggesting that the coordination mechanism of Rh-Hyd with Sn^{2+} is reversible and the Rh-Hyd receptor can be recycled.

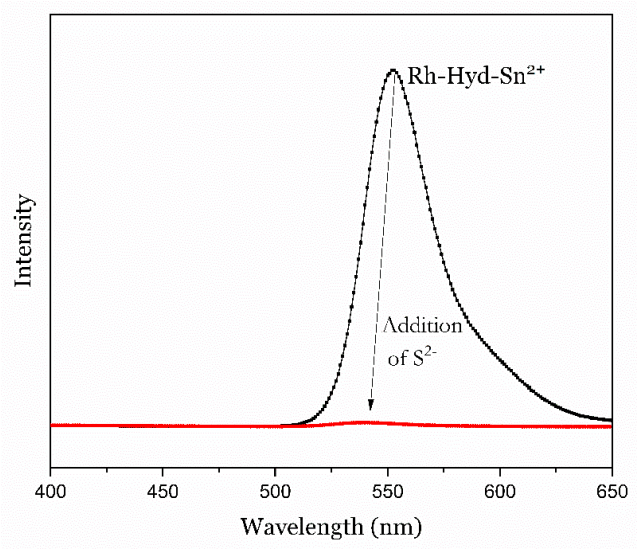

Figure 9. Variations on fluorescence of [Rh-Hyd-Sn^{2+}] by the addition of S^{2-}.

3.4. Potential Application

3.4.1. Imaging Studies by Fluorescent Microscope

To demonstrate the potential application of the receptors, fluorescence imaging experiments were conducted. The Rh-Hyd and its Sn^{2+} complexes (10^{-7} M) were coated on a glass plate and dried at room temperature. The coated films were observed by a Nikon Eclipse E600 microscope equipped with a Nikon C1 confocal unit associated with argon 488 and HeNe 543 lasers. Digital pictures were taken by digital camera at 510 nm wavelength (Figure S12). The imaging results revealed that no fluorescence was observed for the original film (Figure S10a), whereas the apparent fluorescence enhancement was easily observed for their Sn^{2+} complexes (Figure S10b). The receptor can detect Sn^{2+} through visual images, suggesting that the receptor can be used as a test paper or for the imaging of Sn^{2+} in living cells.

3.4.2. Determination of Sn^{2+} from the Catalyzed Reaction Product

In order to illustrate the potential application of the Rh-Hyd for the detection of residual tin in products (impurity), $SnCl_2$ catalyzed reduction reaction of nitrophenol to aminophenol was carried out (Scheme 2). $SnCl_2 \cdot 2H_2O$ (10.0 mmol) was added into a solution of p-nitrophenol (0.967 mmol) in ethanol (5 mL). The mixture was ultrasonicated for 3 h at 30 °C [39]. The solvent was removed by a rotary evaporator. The obtained residue was extracted in dichloromethane, washed with water, and then concentrated (crude; 57%). This crude was further purified by repeated washing by acid and base treatment to yield 4-aminophenol as a white solid. The addition of the Rh-Hyd to the crude ethanolic solution showed a bright red color solution, indicating that Sn^{2+} remained in the crude product as an impurity. In order to determine the total amount of Sn^{2+} in the crude product, the fluorescent intensities of standard Sn^{2+} solution and unknown aminophenol solution were recorded (Figure S11). First, we conducted a titration of $SnCl_2$ solution of known concentration with Rh-Hyd. Then the ethanolic solution of the crude (63 mg along with buffer solution = total 1 mL) was titrated with Rh-Hyd probe. By plotting the fluorescent intensity of known solutions against the concentration of $SnCl_2$ in ppm, the concentration of the $SnCl_2$ in the solution was determined to be 38.27 ppm according to its fluorescent intensity. It was found that 300.2 ppm Sn remained in the crude product (see supporting information).

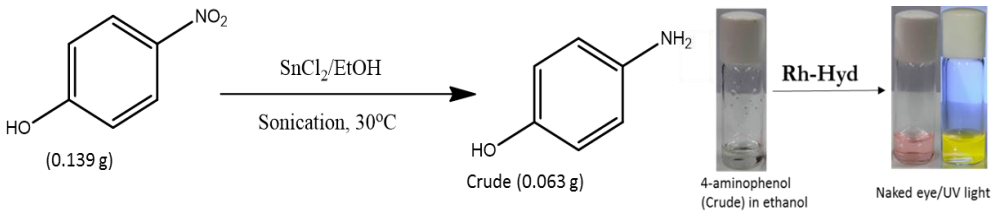

Scheme 2. $SnCl_2$ catalyzed reduction of nitro to amine as an illustration to show the efficiency of Rh-Hyd on the determination of residual tin content.

After further purification, the final product (4-aminophenol) did not exhibit color change and fluorescence with Rh-Hyd, indicating that $SnCl_2$ was completely removed from the final product during purification. It is accepted that $SnCl_2$ is water-soluble and air-sensitive/hygroscopic. Therefore, repeated washing leads to Sn^{2+} free 4-aminophenol. The DLs of fluorescent receptors for Sn^{2+} reported in the literature are listed in Table 1. The data from the table revealed that the Rh-Hyd displays superior detection to Sn^{2+} compared to the reported receptors.

Table 1. Representative sensors with reported LODs.

Reported Sensor for Stannous Ions	LOD	[Ref]
4-(Naphthalen-1-ylethynyl) aniline appended rhodamine (NAP-RD)	5×10^{-9} M	[16]
Rhodamine B and a benzyl 3-aminopropanoate conjugate (RBAP)	0.044×10^{-6} M	[17]
Rhodamine B with N,N-bis-(2-hydroxyethyl)ethylenediamine (R1) and tert-butyl carbazate group (R2) units	5.7×10^{-7} M (R1) and 4.6×10^{-7} M (R2)	[18]
Naphthoquinone–dopamine conjugate	0.1×10^{-6} M	[19]
Benzophenone-based chemosensor	0.3898×10^{-9} M	[20]
Diarylethene with a carbazole	1.9×10^{-3} M	[15]
Rhodamine–amine	1.62×10^{-7} M	This work

4. Conclusions

Besides Hg^{2+}, we have exploited amine-functionalized rhodamine 6G derivatives for the rapid and selective fluorescent detection of Sn^{2+}. The spectral and optical evidence reveals that the carbonyl and amino groups of the receptors are responsible for the coordination with Sn^{2+} and forming 1:1 complexes. The sensitivity and response time of Rh-Hyd towards Sn^{2+} were higher than those of Rh-ED due to the steric limitation to Sn^{2+} coordination and the higher nucleophilicity of hydrazine than ethylene diamine. The LOD of the Rh-Hyd towards Sn^{2+} was 1.62×10^{-7} M, which is much lower than those of most fluorescent receptors reported in the literature. Fluorescent imaging studies demonstrated that the Rh-Hyd could be used to monitor Sn^{2+}. A model Sn^{2+} catalyzed reduction reaction was conducted to evaluate the efficiency of the receptor for the Sn^{2+} impurity in the crude product, which reveals that Rh-Hyd can be a good candidate for the detection of Sn^{2+} in environmental as well as biological samples.

Supplementary Materials: The following supporting information can be downloaded at: https://www.mdpi.com/article/10.3390/chemosensors10020069/s1, Figure S1: ^{1}H-NMR spectrum of Rh-Hyd in $CDCl_3$; Figure S2: ^{13}C-NMR spectrum of Rh-Hyd in $CDCl_3$; Figure S3: ^{1}H-NMR spectrum of Rh-ED in $CDCl_3$; Figure S4: ^{13}C-NMR spectrum of Rh-ED in $CDCl_3$; Figure S5 Mass spectrum of Rh-Hyd; Figure S6: Comparison of ^{1}H-NMR spectra of Rh-Hyd and its complexes with Sn^{2+}; Figure S7: Comparison of ^{13}C-NMR spectra of Rh-Hyd and its complexes with Sn^{2+}; Figure S8: Comparison of ^{1}H-NMR spectra of Rh-ED and its complexes with Sn^{2+}; Figure S9: Comparison of ^{13}C-NMR spectra of Rh-ED in CD_2Cl_2 and its complexes with Sn^{2+} in $CDCl_3$; Figure S10: Fluorescence images of (a) Rh-Hyd and (b) the respective Sn^{2+} complex (magnification 10x); Figure S11: (a) Fluorescent spectra of Rh-Hyd with $SnCl_2$ of known concentration and unknown sample, and (b) calibration curve.

Author Contributions: B.R. designed the experiments and wrote the draft manuscript. V.M. conducted the imaging studies by fluorescent microscope. B.-T.L. evaluated the data and revised the manuscript. All authors have read and agreed to the published version of the manuscript.

Funding: This work was financially supported by the Ministry of Science and Technology, the Republic of China (MOST 110-2221-E-224-034).

Institutional Review Board Statement: Not applicable.

Conflicts of Interest: The authors declare no conflict of interest.

References

1. Elsabbagh, H.S.; Moussa, S.Z.; el-tawil, O.S. Neurotoxicologic Sequelae of Tributyltin Intoxication in Rats. *Pharmacol. Res.* **2002**, *45*, 201–206. [CrossRef] [PubMed]
2. Wang, Q.; Li, C.; Zou, Y.; Wang, H.; Yi, T.; Huang, C. A Highly Selective Fluorescence Sensor for Tin (Sn^{4+}) and its Application in Imaging Live Cells. *Org. Biomol. Chem.* **2012**, *10*, 6740–6746. [CrossRef]
3. Benoy, C.J.; Hooper, P.A.; Schneider, R. TheToxicity of Tin in Canned Fruit Juices and Solid Foods. *Food Cosmet. Toxicol.* **1971**, *9*, 645–656. [CrossRef]
4. Bernardo-Filho, M.; da Conceicão Cunha, M.; de Oliveira Valsa, J.; Caldeira de Araujo, A.; Campos Pereira da Silva, F.; de Souza da Fonseca, A. Evaluation of Potential Genotoxicity of Stannous Chloride: Inactivation, Filamentation and Lysogenic Induction of Escherichia Coli. *Food Chem. Toxicol.* **1994**, *32*, 477–479. [CrossRef]
5. Boogaard, P.; Boisset, M.; Blunden, S.; Davies, S.; Ong, T.; Taverne, J.-P. Comparative Assessment of Gastrointestinal Irritant Potency in Man of Tin(II) Chloride and Tin Migrated from Packaging. *Food Chem. Toxicol.* **2004**, *41*, 1663–1670. [CrossRef]
6. Yang, Y.; Yu, K.; Yang, L.; Liu, J.; Li, K.; Luo, S. One Single Molecule as a Multifunctional Fluorescent Probe for Ratiometric Sensing of Fe^{3+}, Cr^{3+} and Colorimetric Sensing of Cu^{2}+. *Sensors* **2015**, *15*, 49–58. [CrossRef] [PubMed]
7. Yu, C.; Wen, Y.; Zhang, J. Synthesis of a Cu^{2+}-Selective Probe Derived from Rhodamine and Its Application in Cell Imaging. *Sensors* **2014**, *14*, 21375–21384. [CrossRef] [PubMed]
8. Brasca, R.; Onaindia, M.C.; Goicoechea, H.C.; Peña, A.M.d.l.; Culzoni, M.J. Highly Selective and Ultrasensitive Turn-on Luminescence Chemosensor for Mercury (II) Determination Based on the Rhodamine 6G Derivative FC1 and Au Nanoparticles. *Sensors* **2016**, *16*, 1652. [CrossRef]
9. Zhang, Y.; Leng, J. Theoretical Studies on Two-Photon Fluorescent Hg^{2+} Probes Based on the Coumarin-Rhodamine System. *Sensors* **2017**, *17*, 1672. [CrossRef] [PubMed]

10. Zhang, Y.-S.; Balamurugan, R.; Lin, J.-C.; Fitriyani, S.; Liu, J.-H.; Emelyanenko, A. Pd^{2+} Fluorescent Sensors Based on Amino and Imino Derivatives of Rhodamine and Improvement of Water Solubility by the Formation of Inclusion Complexes with β-Cyclodextrin. *Analyst* **2017**, *142*, 1536–1544. [CrossRef]
11. Balamurugan, R.; Liu, J.-H.; Liu, B.-T. A Review of Recent Developments in Fluorescent Sensors for the Selective Detection of Palladium Ions. *Coord. Chem. Rev.* **2018**, *376*, 196–224. [CrossRef]
12. Zhu, L.; Yang, J.; Wang, Q.; Zeng, L. Highly Selective Fluorescent Probe for the Detection of Tin (IV) Ion. *J. Lumin.* **2014**, *148*, 161–164. [CrossRef]
13. Mahapatra, A.K.; Manna, S.K.; Mandal, D.; Mukhopadhyay, C.D. Highly Sensitive and Selective Rhodamine-Based "Off–On" Reversible Chemosensor for Tin (Sn^{4+}) and Imaging in Living Cells. *Inorg. Chem.* **2013**, *52*, 10825–10834. [CrossRef] [PubMed]
14. Cheng, J.; Yang, E.; Ding, P.; Tang, J.; Zhang, D.; Zhao, Y.; Ye, Y. Two Rhodamine Based Chemosensors For Sn^{4+} and the Application in Living Cells. *Sens. Actuators B Chem.* **2015**, *221*, 688–693. [CrossRef]
15. Qu, S.; Zheng, C.; Liao, G.; Fan, C.; Liu, G.; Pu, S. A Fluorescent Chemosensor for Sn^{2+} and Cu^{2+} Based on a Carbazole-Containing Diarylethene. *RSC Adv.* **2017**, *7*, 9833–9839. [CrossRef]
16. Adhikari, S.; Ghosh, A.; Guria, S.; Sahana, A. A Through Bond Energy Transfer Based Ratiometric Probe for Fluorescent Imaging of Sn^{2+} Ions in Living Cells. *RSC Adv.* **2016**, *6*, 39657–39662. [CrossRef]
17. Bao, X.; Cao, X.; Nie, X.; Jin, Y.; Zhou, B. RBAP, a Rhodamine β-Based Derivative: Synthesis, Crystal Structure Analysis, Molecular Simulation, and Its Application as a Selective Fluorescent Chemical Sensor for Sn^{2+}. *Molecules* **2014**, *19*, 7817–7831. [CrossRef]
18. Lan, H.; Wen, Y.; Shi, Y.; Liu, K.; Mao, Y.; Yi, T. Fluorescence Turn-On Detection of Sn^{2+} in Live Eukaryotic and Prokaryotic Cells. *Analyst* **2014**, *139*, 5223–5229. [CrossRef]
19. Ravichandiran, P.; Prabakaran, D.S.; Bella, A.P.; Boguszewska-Czubara, A.; Masłyk, M.; Dineshkumar, K.; Johnson, P.M.; Park, B.-H.; Han, M.-K.; Kim, H.G.; et al. Naphthoquinone-Dopamine Linked Colorimetric and Fluorescence Chemosensor for Selective Detection of Sn^{2+} Ion in Aqueous Medium and Its Bio-Imaging Applications. *ACS Sustain. Chem. Eng.* **2020**, *8*, 10947–10958. [CrossRef]
20. Jadhav, A.G.; Shinde, S.S.; Lanke, S.K.; Sekar, N. Benzophenone Based Fluorophore for Selective Detection of Sn_{2+} Ion: Experimental and Theoretical Study. *Spectrochim. Acta A* **2017**, *174*, 291–296. [CrossRef]
21. Ravichandiran, P.; Krishnamoorthi Kaliannagounder, V.; Antony Paulraj, B.; Boguszewska-Czubara, A.; Masłyk, M.; Pant, H.; Park, C.; Johnson, P.; Park, B.-H.; Han, M.-K.; et al. Simple Colorimetric and Fluorescence Chemosensing Probe for Selective Detection of Sn^{2+} Ions in an Aqueous Solution: Evaluation of the Novel Sensing Mechanism and Its Bioimaging Applications. *Anal. Chem.* **2021**, *93*, 801–811. [CrossRef] [PubMed]
22. Meng, X.; You, L.; Li, S.; Sun, Q.; Luo, X.; He, H.; Wang, J.; Zhao, F. An ICT-Based Fluorescence Enhancement Probe for Detection of Sn^{2+} in Cancer Cells. *RSC Adv.* **2020**, *10*, 37735–37742. [CrossRef]
23. Kong, Y.; Wang, M.; Lu, W.; Li, L.; Li, J.; Chen, M.; Wang, Q.; Qin, G.; Cao, D. Rhodamine-Based Chemosensor for Sn^{2+} Detection and its Application in Nanofibrous Film and Bioimaging. *Anal. Bioanal. Chem.* **2022**, *414*, 2009–2019. [CrossRef]
24. Wang, X.; Song, H.; Fan, C.; Pu, S. Europium(III) Complex Fluorescent Sensor for Dual Channel Recognition of Sn^{2+} And Cu^{2+} Ions in Water. *Spectrochim. Acta A* **2021**, *250*, 119373. [CrossRef] [PubMed]
25. Salem, J.K.; El Nahhal, I.M.; Shurrab, M.H. Citrate Stabilised Silver Nanoparticles as Sensing Probe for In-Situ Sn^{2+} Ion Determination. *Int. J. Environ. Anal. Chem.* **2020**, 1–11. [CrossRef]
26. Ma, X.; Tan, Z.; Wei, G.; Wei, D.; Du, Y. Solvent Controlled Sugar–Rhodamine Fluorescence Sensor for Cu^{2+} Detection. *Analyst* **2012**, *137*, 1436–1439. [CrossRef]
27. Rathinam, B.; Chien, C.-C.; Chen, B.-C.; Liu, J.-H. Fluorogenic and Chromogenic Detection of Cu^{2+} And Fe^{3+} Species in Aqueous Media by Rhodamine–Triazole Conjugate. *Tetrahedron* **2013**, *69*, 235–241. [CrossRef]
28. Wang, S.; Ding, H.; Wang, Y.; Fan, C.; Tu, Y.; Liu, G.; Pu, S. An "Off–On–Off" Sensor for Sequential Detection of Cu^{2+} and Hydrogen Sulfide Based on A Naphthalimide–Rhodamine β Derivative and its Application in Dual-Channel Cell Imaging. *RSC Adv.* **2018**, *8*, 33121–33128. [CrossRef]
29. Yang, Z.; She, M.; Yin, B.; Cui, J.; Zhang, Y.; Sun, W.; Li, J.; Shi, Z. Three Rhodamine-Based "Off–On" Chemosensors with High Selectivity and Sensitivity for Fe^{3+} Imaging in Living Cells. *J. Org. Chem.* **2012**, *77*, 1143–1147. [CrossRef]
30. Han, X.; Wang, D.-E.; Chen, S.; Zhang, L.; Guo, Y.; Wang, J. A New Rhodamine-Based Chemosensor for Turn-On Fluorescent Detection of Fe^{3+}. *Anal. Methods* **2015**, *7*, 4231–4236. [CrossRef]
31. Balamurugan, R.; Chang, W.-I.; Zhang, Y.; Fitriyani, S.; Liu, J.-H. A Turn-On Fluorescence Chemosensor Based on a Tripodal Amine [tris(pyrrolyl-α-methyl)amine]-rhodamine Conjugate for the Selective Detection of Zinc Ions. *Analyst* **2016**, *141*, 5456–5462. [CrossRef] [PubMed]
32. Roy, A.; Das, S.; Sacher, S.; Mandal, S.K.; Roy, P. A Rhodamine Based Biocompatible Chemosensor for Al^{3+}, Cr^{3+} and Fe^{3+} Ions: Extraordinary Fluorescence Enhancement and a Precursor for Future Chemosensors. *Dalton Trans.* **2019**, *48*, 17594–17604. [CrossRef] [PubMed]
33. Hong, M.; Chen, Y.; Zhang, Y.; Xu, D. A Novel Rhodamine-Based Hg^{2+} Sensor with a Simple Structure and Fine Performance. *Analyst* **2019**, *144*, 7351–7358. [CrossRef] [PubMed]
34. Li, D.; Li, C.-Y.; Qi, H.-R.; Tan, K.-Y.; Li, Y.-F. Rhodamine-Based Chemosensor for Fluorescence Determination of Trivalent Chromium Ion in Living Cells. *Sens. Actuators B Chem.* **2016**, *223*, 705–712. [CrossRef]

35. Rathinam, B.; Liu, B.-T. Highly Efficient Probe of Dinuclear Zinc Complexfor Selective Detection of Oxalic Acid. *J. Taiwan Inst. Chem. Eng.* **2021**, *127*, 349–356. [CrossRef]
36. Wang, D.; Xiang, X.; Yang, X.; Wang, X.; Guo, Y.; Liu, W.; Qin, W. Fluorescein-Based Chromo-Fluorescent Probe for Zinc in Aqueous Solution: Spirolactam Ring Opened or Closed? *Sens. Actuators B Chem.* **2014**, *201*, 246–254. [CrossRef]
37. Kraithong, S.; Damrongsak, P.; Suwatpipat, K.; Sirirak, J.; Swanglap, P.; Wanichacheva, N. Highly Hg^{2+}-Sensitive and Selective Fluorescent Sensors in Aqueous Solution and Sensors-Encapsulated Polymeric Membrane. *RSC Adv.* **2016**, *6*, 10401–10411. [CrossRef]
38. Johnson, A.D.; Curtis, R.M.; Wallace, K.J. Low Molecular Weight Fluorescent Probes (LMFPs) to Detect the Group 12 Metal Triad. *Chemosensors* **2019**, *7*, 22. [CrossRef]
39. Gamble, A.B.; Garner, J.; Gordon, C.P.; O'Conner, S.M.J.; Keller, P.A. Aryl Nitro Reduction with Iron Powder or Stannous Chloride under Ultrasonic Irradiation. *Synth. Commun.* **2007**, *37*, 2777–2786. [CrossRef]